J Mater Sci (2006) 41:8226–8243
DOI 10.1007/s10853-006-0879-9

The efficiency of various toughening agents in novel phenolic type thermoset resin systems

T. Dipl.-Ing. Gietl · H. Dr.-Ing. Lengsfeld · V. Dr.-Ing. Altstädt

Received: 20 April 2005 / Accepted: 1 November 2005 / Published online: 1 October 2006

Abstract Two novel phenolic type thermosetting resin systems are investigated regarding the effectiveness of different toughness modifiers. These modifiers derive from different groups such as elastomers, thermoplastics, and core–shell polymers. Measurements are accomplished by mechanical, thermal, and microscopical studies. Toughness improvement is determined by increasing K_{Ic} and G_{Ic} values while glass transition temperature, flexural strength, and modulus must not suffer greatly. Suggestions on the mechanisms of toughness modification in the novel resins are made based on images from scanning electron microscopy.

Introduction

Although nowadays epoxy resins and their properties belong to everyday life, the demand for even better matrix and prepreg systems in aerospace industry forces research in other chemistries. Disadvantages of epoxy resins such as shrinkage during cure, long curing schedules, high curing temperatures, moisture absorption, and poor stress–strain performance, among others, must be overcome.

The fundamental understanding of the present paper is that a recently developed class of a phenolic-type resin system can meet these wishes, i.e., better matrix and composite properties. These benzoxazine resins provide such desirable properties as heat resistance, good electronic performance, and flame retardance. Additionally, problems like high water absorption and dimensional instability during cure are overcome. Furthermore, the preparation of the experimental resins does not require strongly acidic or basic catalysts and no by-products are produced during polymerization [1].

In order to gain widespread acceptance the resin must meet crucial criteria such as outstanding performance, low cost, and acceptable processing characteristics by the conventional techniques currently used in industry. The benzoxazine monomer can be prepared easily from inexpensive raw materials and hence the resins are expected to compete with epoxy resins and various phenolic resins in performance and costs. Due to the aromatic polymer backbone and the extensive inter- and intra-molecular hydrogen bonding, the physical, mechanical, and thermal properties are excellent which is crucial for future applications in aerospace, automotive, and industry technologies. The production of a benzoxazine monomer is shown in Fig. 1.

However, due to the inherent brittleness of the novel resins, effective and compatible toughness modifiers must be found. Therefore the goal of the present work was to investigate the efficiency of various

T. Dipl.-Ing. Gietl (✉)
Competence Center Sealing Technology, Schaeffler KG, Industriestrasse 1–3, Herzogenaurach 91074, Germany
e-mail: thomas.gietl@schaeffler.com

H. Dr.-Ing. Lengsfeld
Technology Part Production, Airbus Germany, Ottenbecker Damm, Stade 21684, Germany
e-mail: hauke.lengsfeld@airbus.com

V. Dr.-Ing. Altstädt
Polymer Engineering, Universität Bayreuth, Universitätsstrasse 30, Bayreuth 95447, Germany
e-mail: volker.altstaedt@uni-bayreuth.de

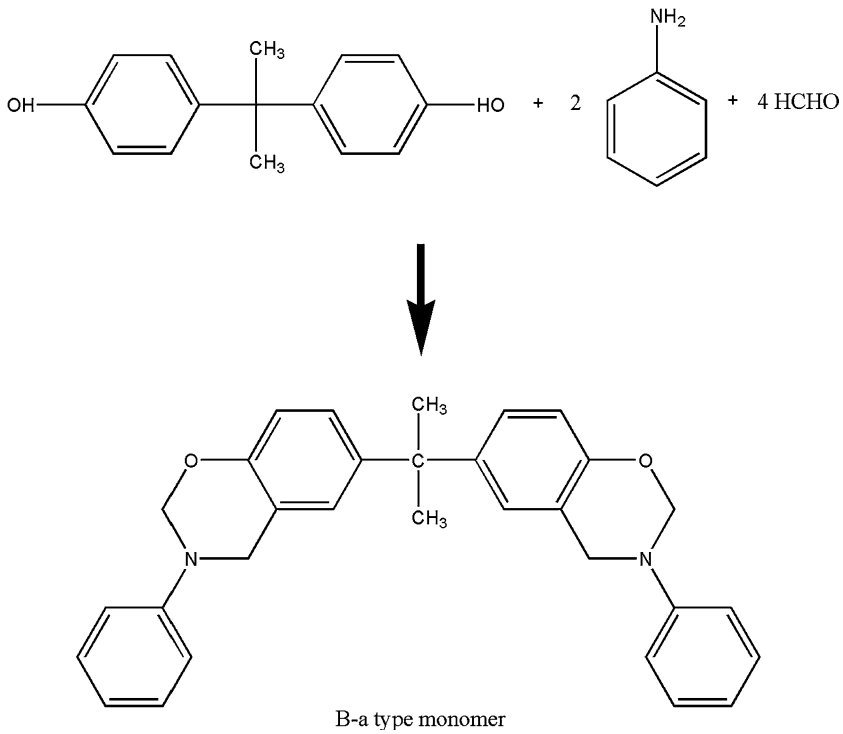

Fig. 1 Structure of B-a type benzoxazine monomer

tougheners in two benzoxazine resins for composites applications, e.g., resin film infusion or resin transfer molding, as well as for adhesive, paste, film, or syntactic foam applications.

The modifiers were chosen according to previous studies with epoxy resins and derive from several material groups: thermoplastics [2], reactive liquid rubbers [3–7], and core–shell rubbers [8]. Due to the unfamiliar properties of the benzoxazine resin systems, the addition of modifiers was limited to the neat resins and started out at 10% by weight. Although in the case of the F-a type benzoxazine, an additional 5% of a catalyst was necessary to achieve a complete cure at three hours at 177 °C.

After the miscibility of resin and toughener was determined and the properties of the samples were studied, it was decided whether further investigation of certain modifiers was reasonable either at 5% or 20% depending on the previous results. The performance of the tougheners was evaluated by formulating the neat resin with each predetermined modifier. Their influence is measured under the following criteria:

High glass transition temperature
High flexural strength and modulus
High fracture toughness
Low water absorption
Perpetuation of low viscosity at moderate processing temperatures.

Experimental procedure

Materials

The materials used in this investigation derive from the B-a type benzoxazine whose structure and production is presented in Fig. 1.

In Fig. 2, a drawing is presented about the principal ring-opening polymerization of benzoxazines [9].

The structure of the investigated F-a type benzoxazine resin by Shikoku Chemicals Corporation, Japan is shown in Fig. 3.

The polybenzoxazines shown here are a novel class of ring-opening thermoset resins with key characteristics like near-zero shrinkage and no by-product release upon polymerization. No strongly acidic or basic catalysts are necessary upon curing. Furthermore, the resins feature low water absorption as well as superior electrical and self-fire-extinguishing properties. In the case of the F-a type benzoxazine, the usage of the 4,4′-thiobis-phenol catalyst (Fig. 4) allowed a complete cure at the desired time–temperature conditions.

Previous tests at Henkel Loctite Aerospace using differential scanning calorimetry (DSC) and dynamic mechanical thermal analysis (DMTA) methods determined the most suitable ratio of catalyst in the resin. A particle size analysis showed a broad distribution in the

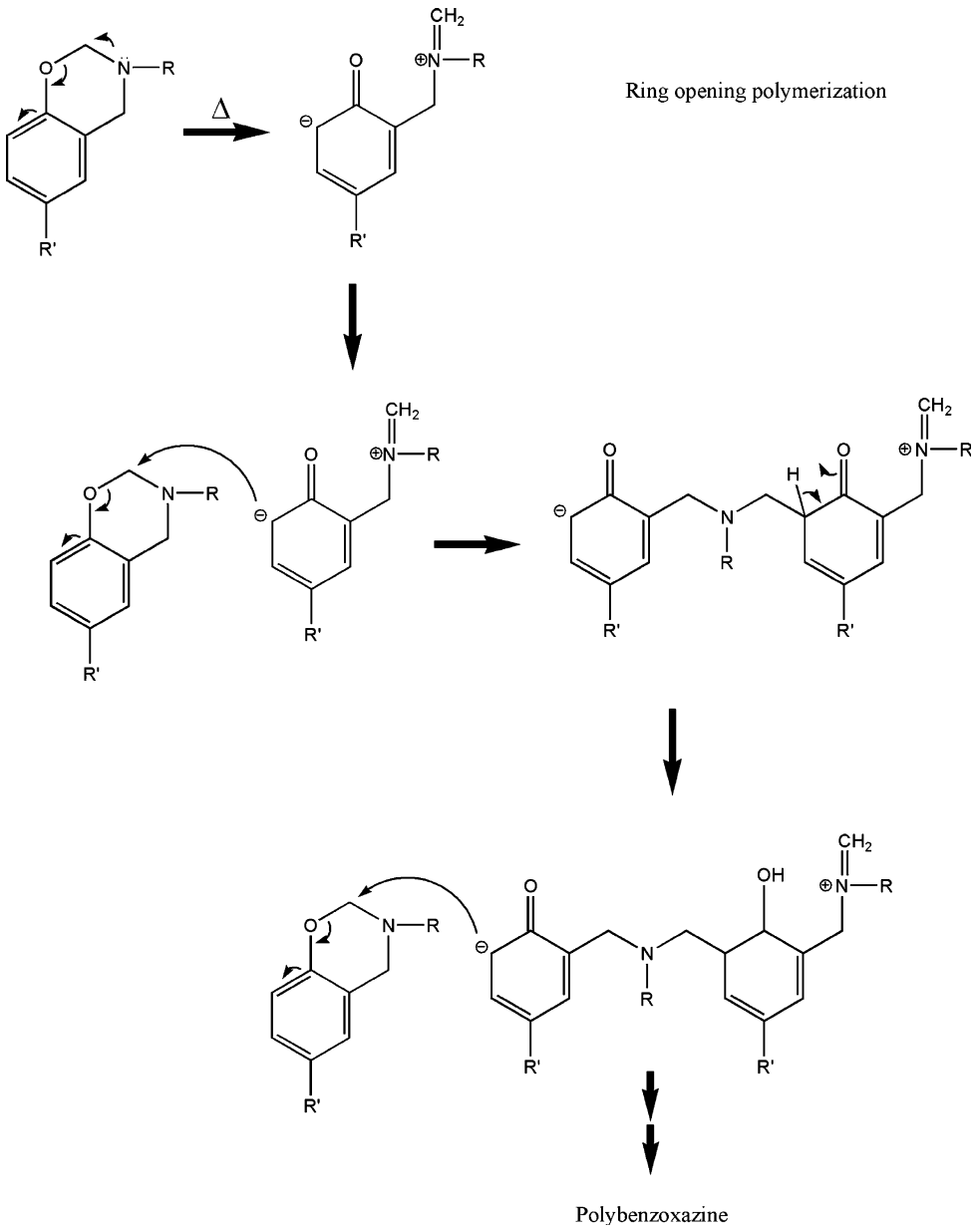

Fig. 2 Schematic drawing of the ring-opening mechanism for the polymerization of polybenzoxazines

powder between a few micrometers up to more than 1,000 μm with a mean of 186 μm. The powder was used as received.

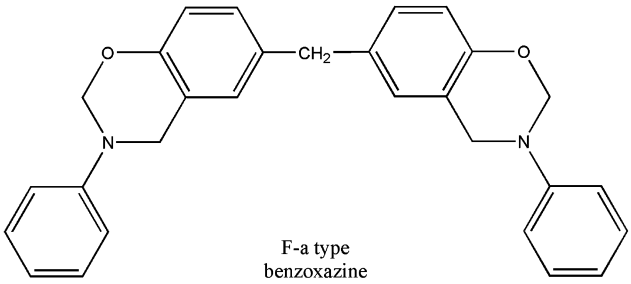

Fig. 3 Production and structure of F-a type benzoxazine monomer

Further, the B-m type benzoxazine was investigated as a second derivative of the novel resins. Fig. 5 shows its structure [9].

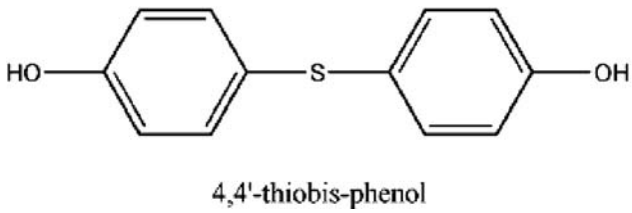

Fig. 4 Structure of catalyst for EB-1 resin

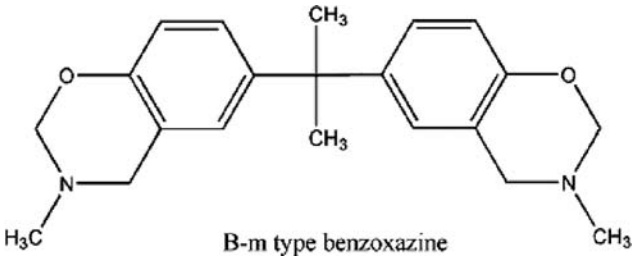

Fig. 5 Structure of B-m type benzoxazine monomer

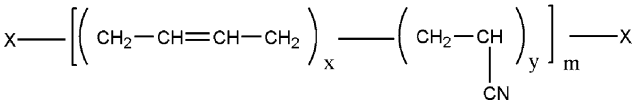

Fig. 6 X-terminated reactive liquid rubber

One of the reactive liquid rubbers used (see Fig. 6) was the amino-terminated butadiene–acrylonitrile rubber (ATBN) HYCAR® ATBN 1300x16 from former B.F. Goodrich Company [10].

HYCAR® CTBN 1300x13 was the second liquid rubber to be studied as a toughening agent, also supplied by former B.F. Goodrich Company. It is a liquid copolymer of butadiene and acrylonitrile with carboxyl end groups (CTBN) [10]. The manufacturer's published properties for these liquid rubbers are shown in Fig. 7.

The amine-terminated rubber is prepared by reacting the carboxyl-terminated rubber with *N*-aminoethylpiperazine. The former had a higher reactivity and molecular weight, but otherwise both rubbers were the same [11].

Three core–shell polymers were studied in their toughening abilities; two of them are commercially available chemicals while the third is a laboratory scale product.

Rohm & Haas Company kindly supplied the poly(butadiene–methylmethacrylate) copolymer Paraloid™ EXL 2330 in powder form with a particle size distribution between 10 and 500 μm and a mean of 161 μm.

Kaneka Texas Corporation supplied a methylmethacrylate–acrylic copolymer named Kane Ace M580. The product was also delivered as a powder and had a similar particle size distribution with a mean of 184 μm.

The laboratory scale core–shell polymer (CSR-3) was pre-reacted with the experimental resin by the supplier. This butadiene–acrylic copolymer consisted of a rubbery core inside a glassy, rigid shell and was incorporated in the neat F-a type polybenzoxazine at a ratio of 26.5% by weight. The average particle size may be assumed to be around 100 nm with a very small distribution.

As a thermoplastic toughener the poly 2,6-dimethyl-1,4-phenylene oxide (PPO) PPO® SA120 from General Electric Company was used. The solid granulate was ground by hand to a powder of 19 μm mean size with a maximum of 55 μm. The material had a number molecular weight M_w of 2,350 g/mol and an intrinsic viscosity of 0.12 dl/g. Figure 8 shows the generic structure of the plastic.

Another thermoplastic used was a laboratory-scale hydroxyl-terminated polyether sulfone (PES) similar to the commercially available PES grades. The polymer is shown in Fig. 9.

The polymer had an average number molecular weight M_w of 4,200 g/mol and a particle size with a mean of 17.5 μm with a maximum of 70 μm.

For the incorporation of PES, dimethylformamide was chosen as a solvent.

The molds used for the production of all samples were coated with FREKOTE® 700-NC mold release agent by Loctite®. The mold surface was covered with a thin layer of the clear silicon based liquid by moistening with a clean cloth.

Fig. 7 Properties of Hycar® polymers [5]

Hycar Polymers	ATBN 1300x16	CTBN 1300x13
Acrylonitrile Content, %	18	26
Carboxyl Content: Acid Number	-	32
EPHR*	-	0.057
Amine Equivalent Weight (AEW)	900±10	-
Amine Value	62	-
Brookfield Viscosity, mPas or cP, @ 81°F (27°C)	200,000±50,000	500,000±140,000
Solubility Parameter**	-	9.15
Molecular Weight, Mn	-	3150
Glass Transition Temperature, °C***	-51	-39

* Equivalents per hundred rubber
** Calculations based on molar attraction constants
*** Measured via DSC

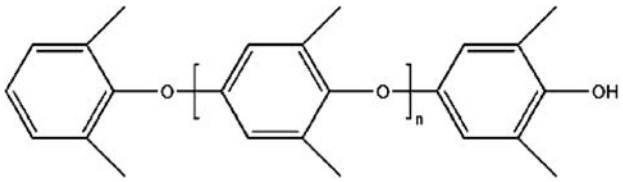

PPO® Resin

Fig. 8 Generic structure of PPO®

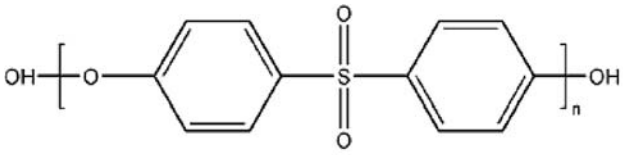

hydroxyl-terminated poly(ether sulphone)

Fig. 9 Laboratory grade PES

Measurements

DSC was done with a Perkin-Elmer DSC 7. The heating rate was 10 °C/min for the first of each sample run and 40 °C/min for the second. Both tests were performed under nitrogen. An amount of 5–8 mg of each sample was weighed into a small aluminum pan and covered with a lid.

Particle size distributions were performed on a Coulter LS particle size analyzer with an LS 230 dry powder module.

Gel times were measured with only a few samples using a Fisher–Johns melting point apparatus at 177 °C. The gel point was determined as soon as it was no longer possible to pull vertical strings of the resin with a sharpened wooden stick.

Thermal gravimetric analysis (TGA) was done on a Perkin-Elmer Pyris 1 to determine volatiles in mixtures prepared via solvent route. The samples were tested under air between 40 and 300 °C at a heating rate of 5 °C/min.

Fourier transformed infra red (FTIR) tests were done on a Nicolet Smart Miracle Avatar 360 with a Zn/Se cell to quickly proof the conformity of two samples.

All samples were cured as open surface castings under pressure in a Lipton autoclave with a volume of 4.45 m^3. The program of the cycle started with the pressure build-up to a maximum of 6.2 bar, was followed by a 1 h ramp from 32 to 177 °C, i.e., 2.4 °C/min, was held for 3 h at that temperature, and finished with a 1 h ramp down to 32 °C whereupon the pressure was released. This curing technique usually applied with composite materials was found to deliver excellent results likewise for neat resin plates in previous studies [12].

A Buehler Ecomet 3 Variable Speed Grinder-Polisher was used at 180–270 rpm to finish the specimens.

DMTA was done with a Rheometrics Scientific DMTA IV. The samples with the size of 27.94 mm × 12.7 mm × 1.6 mm were tested in a single point bending mode at a frequency of 1 Hz with a heating rate of 5 °C/min. The temperature range started at 40 °C for all systems. The EB-2 systems were heated up to 250 °C while the EB-1 systems were stopped at 220 °C. The strain setting applied was 0.1%.

The absorption of moisture which relates directly to the hot/wet T_gs was determined by putting the DMTA specimens for 3 days into boiling distilled water prior to testing. The samples were weighed with a Mettler Toledo PR 5002 scale accurate to 0.01 g before and after the soaking cycle. Samples were taken out of the water bath, excessive water was removed with an absorbant cloth, and the specimens were immediately tested under the conditions mentioned above.

The specimens mechanically tested in a three-point bending mode were prepared following the standard test methods for flexural properties of unreinforced and reinforced plastics and electrical insulating materials in ASTM D 790-97 [13]. The resin sheets were cut into 12.7 mm wide strips with a water-cooled diamond wheel blade. These strips were sanded to the desired length and thickness according to the purpose of the specimen. According to ASTM D 790-97 [13], the flexural strength was determined in a three-point bending test with specimens requiring minimum dimensions of 7.62 mm span, 12.7 mm width, and 2.8–4.1 mm thickness. The flexural strength equals the maximum fiber stress in the outer fibers at the moment of break. Hence, a homogeneous elastic material is tested in flexure as a simple beam supported at two points and loaded at the midpoint. The maximum stress in the outer fibers occurs at the midspan. The maximum stress was calculated at the point of break from the load–deflection curve by Eq. 1 (maximum fiber stress):

$$S = \frac{3PL}{2bd^2}, \tag{1}$$

where S is the stress in the outer fibers at midspan in MPa, P the load at the point of failure on the load–deflection curve in N, L the support span in mm, b the width of the beam tested in mm, and d is the depth of the beam tested in mm. The crosshead speed of the testing machine was 1.27 mm/min and transducers with 445 or 2,224 N were used.

Further in ASTM D 790-97 [13], the determination of a modulus of elasticity, often called ‘‘flexural

modulus'', is described. It is possible by drawing a tangent to the steepest initial straight-line portion of the load–deflection curve and using Eq. 2 (modulus of elasticity (flexural modulus)):

$$E_{\mathrm{H}} = \frac{L^3 m}{4bd^3}, \tag{2}$$

where E_{H} is the modulus of elasticity in bending in MPa, L the support span in mm, b the width of beam tested in mm, d the depth of beam tested in mm, and m is the slope of the tangent to the initial straight-line portion of the load–deflection curve in N/mm of deflection. The tangent modulus of elasticity is the ratio, within the elastic limit, of stress to corresponding strain.

Plane-strain fracture toughness and strain energy release rates were determined as described in ASTM D 5045-96 [14]. Single edge notch bending (SENB) specimens with the dimensions shown in parentheses were prepared (56 mm × 13 mm × 3.5 mm). Testing was done at a constant displacement rate of the crosshead at 1.016 mm/min with a load cell of 445 N maximal value capacity. The support span was 51 mm. Both of these tests were done at room temperature with a screw-driven United test frame.

The specimen had a length of 51.31 mm, a width of 12.7 mm, and a thickness between 2.8 and 4.1 mm. First, a notch was milled in the specimen as shown in the standard with a two-flute HSS end mill of 1.59 mm diameter using a vertical mill. Then, by tapping with a fresh razor blade, a straight propagating crack was initiated. This resulted in a natural character of the crack since it started ahead of the blade. Special attention was paid to the a/W ratios of all specimens as by this ratio the validity of linear elastic fracture mechanics is ruled [14].

Researchers as well as industry workers frequently refer to the strain energy release rate. The ASTM standard offers a conversion to the strain energy release rate using Eq. 3 (relation between G_{Ic} and K_{Ic})

$$G_{\mathrm{Ic}} = \frac{(1-\nu^2)K_{\mathrm{Ic}}^2}{E} \tag{3}$$

In Eq. 3 G_{Ic} is the strain energy release rate in J/m^2, ν the Poisson ratio that in the given case was set at 0.35 due to investigations in failure of brittle plastics by Bucknall [15], K_{Ic} the measured plane-strain fracture toughness in $\mathrm{MPa}\sqrt{\mathrm{m}}$ and E stands for the Young's modulus. Since the preparation of specimens for determination of tensile properties was only performed for some specific samples in this project, the flexural modulus was used instead of the Young's modulus in Eq. 3. The authors are well aware that the received G_{Ic} values are not to be used as an absolute quantitative number, but since all resin systems were examined by the same methods, a comparison within the present project is assumed to be accurate enough. It was ensured that the flexural modulus was determined under the same test conditions that applied for the testing of the SENB specimens.

Scanning electron microscope (SEM) images were done using the JEOL JSM-5600. The electron acceleration was set at 20 kV. Specimens were sputtered with gold–palladium.

Sample preparation

Since the preparation of the samples varied depending on the modifier to be incorporated the method applicable is described in detail. The various amounts of resin and toughener are listed in Figs. 10 and 11.

Fig. 10 Table of sample formulations: neat, rubber modified, and PES modified resins

Formulation	EB-1	EB-2	A-EB-1	A-EB-2	A-EB-2+	C-EB-1	EB-1PES	EB-2PES
F-a type benzo.	95		85.5			85.5	90.25	
Catalyst	5		4.5			4.5	4.75	
B-m type benzo.		100		90	80			90
ATBN			10	10	20			
CTBN						10		
PES							5	10

Fig. 11 Table of various sample formulations: PPO® and core–shell modified resins

Formulation	EB-1SA120	EB-2SA120	EB-2SA120+	EB-1M580	EB-1EXL	EB-2EXL	CSR-3
F-a type benzo.	85.5			86.1	86		73.5
Catalyst	4.5			4.3	4.4		
B-m type benzo.		90	80			90	
PPO SA120	10	10	20				
Kane Ace M580				9.6			
Paraloid EXL 2330					9.6	10	
CSR-3							26.5

All resin mixtures were cast onto rectangular aluminum molds as sheets with a thickness of 3.175 mm. The mold surface was coated with a thin layer of Frekote® 700-NC to assure easy release of the cured resins.

The EB-1 system was mixed with 95% F-a type benzoxazine and 5% catalyst. The solid F-a type benzoxazine was used as received and heated in an oven at 93 °C until it liquefied. Then 5% of 4,4′-thiobis-phenol catalyst was added in powder form with a mean particle size of 186 μm and dissolved in the resin, keeping the mixture liquid at 93 °C. The mixture was degassed in a vacuum oven at 93 °C for 15–30 min before it was poured into the preheated mold. Then the mixture was allowed to cool down to room temperature before it was cured in the autoclave.

The preparation of the EB-2 system was done at 100 °C without any catalyst.

The method for the addition of liquid rubber tougheners followed the previously described preparation of the EB-1 resin through the degassing step. Then, at 93 °C, the ATBN or CTBN was weighed directly into the mixture. To disperse the rubber homogeneously the mixture was heated and stirred alternately for 15 min before it was poured into the preheated mold. The samples were called A-EB-1 for the ATBN added and C-EB-1 for the CTBN added resin.

The A-EB-2 resin was prepared at 100 °C with 90% EB-2 resin and 10% ATBN. The A-EB-2+ system contained 80% resin and 20% rubber. CTBN samples were not made with the B-m type benzoxazine due to disappointing test results with the F-a type benzoxazine.

EB-1PES was mixed from 95% F-a type benzoxazine and 5% of an experimental grade PES.

Screening tests strongly recommended the investigation of a solvent route to insert the thermoplastic into both resins. The experimental grade PES by BASF AG Germany and the F-a type benzoxazine were separately dissolved in dimethylformamide (DMF) at a ratio of 1:1. To accelerate the process, the materials were heated inside an oven at 71 °C. Both mixtures were stirred several times until clear fluids remained. Then the container with the PES was emptied into the benzoxazine solution and mixed well. This mixture was then transferred to a rotary evaporator to remove the solvent. The rotating flask was heated in an oil bath at 113 °C and evacuated. After the solvent was removed, a homogeneous yellowish mixture remained at the bottom of the flask. Above, a separate ring of darker yellowish color remained stuck to the flask. The solidified resin parts were tested by FTIR and by TGA to study the homogeneity and the amount of trapped solvent. DMTA specimens were cured.

With the EB-2PES an attempt was made to incorporate 10% of the toughener in the B-m type benzoxazine also using the methods described above. DMTA and K_{Ic}/G_{Ic} specimens were cured.

The material ratios of the mixtures described below can be seen in Fig. 11.

For the preparation of the EB-1SA120 system 10% of the toughener PPO® SA120 was mixed into the EB-1. The same ratio was used with the EB-2SA120 resin. An amount of 20% toughener was used in the EB-2SA120+ system.

The incorporation of this thermoplastic toughener was done by mixing the grounded granulate of 19 μm mean particle size with the EB-1 resin. The mixture was heated and stirred for 15 min at 107 °C and afterwards poured into the preheated mold. The same method was applied to the EB-2 resin.

Three different core–shell polymers were studied in their toughening abilities of the F-a type benzoxazine and one of them also in the B-m type. The Kane Ace M580 was investigated as a commercially available core–shell product. It was mixed with the EB-1 system only.

The also commercially available core–shell product Paraloid™ EXL 2330 was mixed with EB-1 and EB-2 resin.

The Kane Ace M580 and the Paraloid™ EXL 2330 were both added at high shear rate with a homogenizer. The benzoxazine resins in both cases were mixed with the powdery core–shell polymers of 160–185 μm mean particle size before the catalyst was added in case of the F-a type. By applying a high shear rate the resin remained liquid while the core–shell particles were laced in with a funnel. The temperature of the mixtures remained around 99 °C. After the powder was well dispersed, the stirrer was removed and the catalyst was added at 107 °C. Due to the tarnish of the resin it could not be observed the catalyst had completely dissolved. Therefore it was alternately heated and stirred for approximately half an hour and then the mixture was cast into the preheated mold.

The CSR-3 sample was prepared by a third party at a ratio of 73.5% neat F-a type benzoxazine and 26.5% of a laboratory scale core–shell product. It was used as received and due to the high amount of core–shell rubber in the resin it had a significantly higher viscosity compared to all the other resins studied. Hence it did not liquefy but rather softened at 93 °C. No catalyst was added and the rubbery bulk was placed in the preheated mold and compressed by hand to cover as much surface area as possible.

Results and discussion

The baseline and reference throughout the project was given by the so-called EB-1 system that consisted of F-a type benzoxazine cured with 5% by weight of the 4,4′-thiobis-phenol catalyst. The average T_g was found to be 158 °C for the dry specimens and 143 °C for the wet specimens. The moisture absorbed was 0.9%.

It was found that an increase in concentration of catalyst in the EB-1 resin improved the storage modulus, but at the same time lowered the T_g and led to a higher moisture uptake. The loss of T_g value in the hot/wet properties then was significant.

The relatively new attempt to toughen, for example, epoxy resins with thermoplastic modifiers led to several questions with the benzoxazine resins. While General Electric's PPO® SA120 dissolved in the EB-1 resin forming a separate phase with an average particle size of 1 μm inside the cured resin, the EB-2 system remained clear even when an amount of 20% toughener was added.

Two of the three core–shell polymers studied in this project were mixed into the benzoxazine resins by high shear rate applied with a stirrer. All resins containing these tougheners appeared opaque after curing. The third sample was prepared by a third party and was used as received and appeared opaque as well. The results about the efficiency of core–shell polymers varied with the products and are described more detailed in the following paragraphs.

The incorporation of Hycar® CTBN 1300x13 resulted in a slightly higher average T_g of 161 °C for the dry specimens and 144 °C for the hot/wet conditioned ones. Other than that the cured specimen appeared very brittle.

Hence the most intensely investigated toughness modifier was the ATBN rubber. In the EB-1 system 10% was incorporated, whereas in the EB-2 system 10% and also 20% were studied. The following chapters cover detailed results.

Thermal behavior

All samples were tested via DMTA as described earlier. The results were compared with consideration of the T_gs measured at the knee of the storage modulus curve. In Fig. 12 all temperatures of the dry conditioned specimens are shown in light color while the matching hot/wet conditioned specimens are in a darker color.

It was found with almost no exception that the glass transition in the hot/wet conditioned specimens shifted to lower temperatures in the range of 89–95% of the dry specimens' value. Interesting was that with an increasing content of ATBN rubber in the EB-2 system, the T_g, dry increased and the decline of the T_g, wet was lowered from 97% with 10% toughener to no decline at all when 20% were added. The exact values are shown in Fig. 13.

Similar behavior was found in the PPO® toughened EB-2 resin. Although the T_g, dry decreased by 4 °C, the percentage loss changed from 5% to 2%. In Fig. 14 the numeral values are shown. The EB-1PES is not shown in Fig. 12 since it was tested only as a dry conditioned specimen because the processing of this sample system was done with a low amount of material.

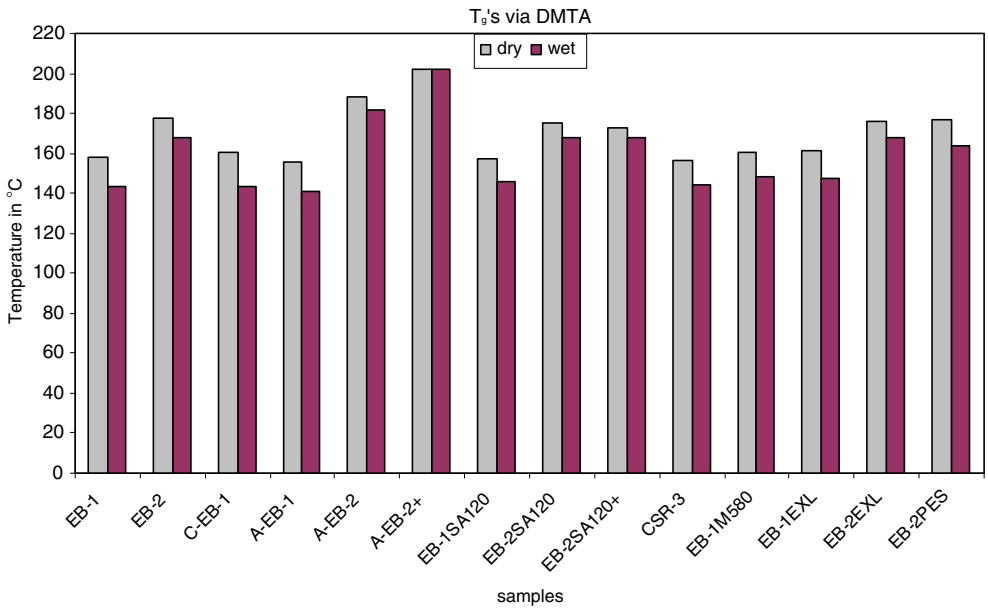

Fig. 12 Glass transition temperatures of dry and hot/wet tested DMTA specimens

Sample	EB-1	EB-2	C-EB-1	A-EB-1	A-EB-2	A-EB-2+
T_g, dry °C	158	177	161	156	188	202
T_g, wet °C	143	168	144	141	182	202

Fig. 13 Glass transition temperatures of neat and rubber toughened benzoxazines in °C

Sample	EB-1SA120	EB-2SA120	EB-2SA120+	EB-1PES	EB-2PES
T_g, dry °C	157	176	172	159	177
T_g, wet °C	146	167	168	N/A	164

Fig. 14 Glass transition temperatures of PPO® and PES toughened benzoxazines in °C

Sample	EB-1M580	EB-1EXL	EB-2EXL	CSR-3
T_g, dry °C	161	161	176	157
T_g, wet °C	148	147	168	144

Fig. 15 Glass transition temperatures of core–shell toughened samples in °C

The T_g, dry was 159 °C and hence did not affect negatively the property of the neat EB-1 resin.

In Fig. 15 the results of the core–shell rubber toughened samples are presented. Note that the CSR-3 contained 26.5% toughener while all other samples contained 10%. It is remarkable that this formulation reached the neat resin's properties in matters of T_g.

An important observation regarding the hot/wet conditioned specimens was their swelling behavior above temperatures around 220 °C which finally led to their decomposition. Apparently the pure formulations of the experimental resins with tougheners caused this behavior. Yet the search for chemical formulations that avoid this behavior far above the target service temperature was not subject of this survey.

Moisture absorption

All specimens absorbed between 0.8% and 1.3% water (Fig. 16). This is significantly lower than the overall absorption of many epoxy resins. While the neat EB-1 resin took up a little less than the neat EB-2 system, it was observed that an increase in weight percentage of ATBN or CTBN rubber also increased the moisture absorption.

A-EB-1 as well as C-EB-1 took up 1.0%, whereas the EB-1 by itself took up 0.90%. In the EB-2 resin an addition of 10% ATBN rubber did not change the amount of absorbed water, but at 20% a significant increase from 1.1% to 1.3% was evident.

The addition of PPO® in the EB-1 system did not change the moisture absorption, but it resulted in a reduction of affiliated water when used in the EB-2 resin, especially when added at the higher quantity of 20%. The uptake decreased from 1.1% to 0.8%.

Different results were measured within the core–shell modifier group. While the EB-1M580, the EB-1EXL, and the EB-2EXL mixtures showed a slight increase in moisture absorption, the CSR-3 containing a significantly higher concentration of core–shell rubber did not change the property of the neat EB-1 resin. It was assumed the rigid and glassy shell sealed the rubbery core and thereby prevented the latter from water absorption.

The EB-2PES showed an increased moisture absorption of 1.3%.

Flexural properties

According to ASTM D 790-97 [13], the flexural strength was determined in a three-point bending test.

In Fig. 17 the values of the flexural strength for each formulation are shown in MPa, values in parenthesis are in ksi. Each value is an average of at least three specimens tested for each formulation. The EB-1 system had a flexural strength of 48 ± 4 MPa while the EB-2 resin started at 87 ± 6 MPa.

The addition of 10 phr of CTBN rubber or ATBN rubber improved the flexural strength of the resins. This behavior was not found in our own tests with tetrafunctional epoxies. Most other workers found significant decreases of strength and modulus when elastomeric tougheners were added [16]. The carboxyl-terminated liquid rubber lifted the value of the C-EB-1 sample to 55 ± 4 MPa while the amino-terminated achieved 66 ± 1 MPa in the EB-1 and 100 ± 41 MPa in the EB-2 resin. An amount of 20 phr ATBN in the EB-2 system lowered this value to 60 ± 6 MPa.

Also, when PES was studied in the EB-2PES system, a compromise in flexural strength was observed (58 ± 3 MPa). This decline of flexural performance disagrees with results found in tetrafunctional epoxy resins, where the modulus remained nearly unaffected [16, 17]. The exact values are also shown in Fig. 17, where the PPO® toughened samples are called EB-1SA120 (39 ± 5 MPa), EB-2SA120 (39 ± 3 MPa), and EB-2SA120+ (20 ± 4 MPa). Contrary to behavior in epoxy resins, the modifier caused a noticeable decrease in flexural properties, especially in the EB-2 system at 20% ratio.

The behavior of the core–shell rubber toughened specimens varied. While the CSR-3 (91 ± 12 MPa) and the Kane Ace M580 (84 ± 18 MPa) mixtures increased

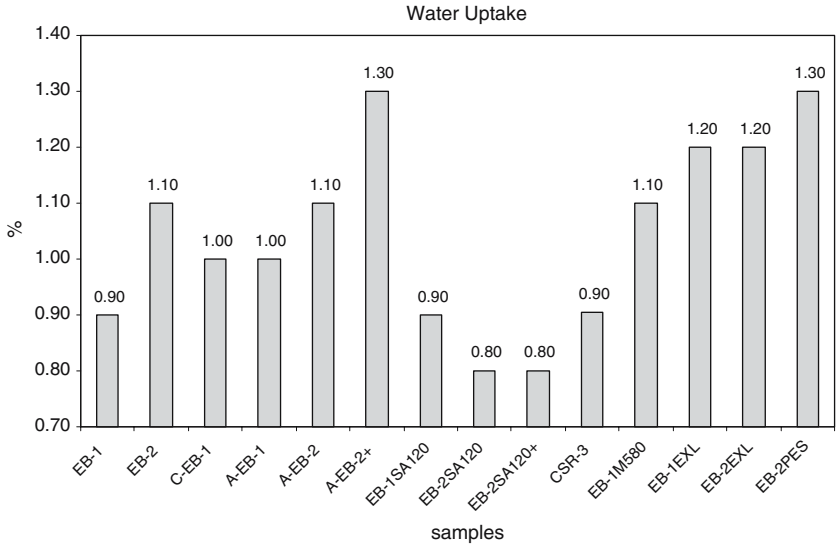

Fig. 16 Moisture absorption of all specimens

the strength of the EB-1 system, the Paraloid™ EXL 2330 increased the strength of the EB-1 system to 53 ± 1 MPa, but decreased it in the EB-2 to 73 ± 8 MPa compared to the neat resins' properties.

As described earlier according to ASTM D 790-97 [13], the determination of a modulus of elasticity was undertaken using the equations given in the technical standard.

Figure 18 shows a loss in flexural modulus of all EB-1-based systems.

Interesting was the difference in flexural modulus performance that was caused by different amounts of PPO® in the EB-2 resin. While 10% of the toughener increased the value to 4.2 ± 0.28 GPa, it remained unchanged by a ratio of 20% compared to the neat resin's property.

All other tougheners lowered the flexural modulus of both benzoxazine resins.

Plane-strain fracture toughness K_{Ic} and strain energy release rate G_{Ic}

The ASTM Standard Test Method D 5045-96 [14] was followed to determine the plane-strain fracture toughness of all evaluated samples. The determined K_{Ic} values are shown in Fig. 19.

The values shown in Fig. 19 are average numbers received from different amounts of specimens. The

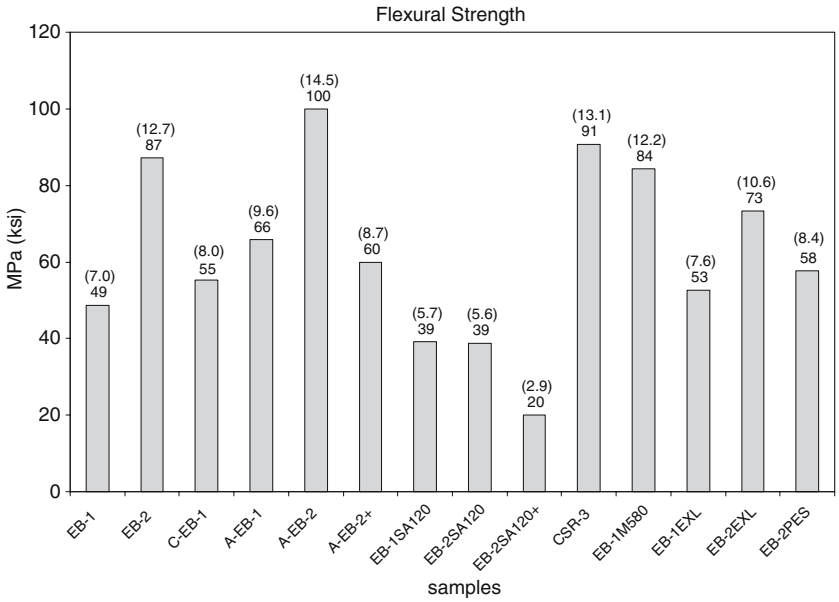

Fig. 17 Flexural strength of all specimens in MPa; values in parentheses in ksi

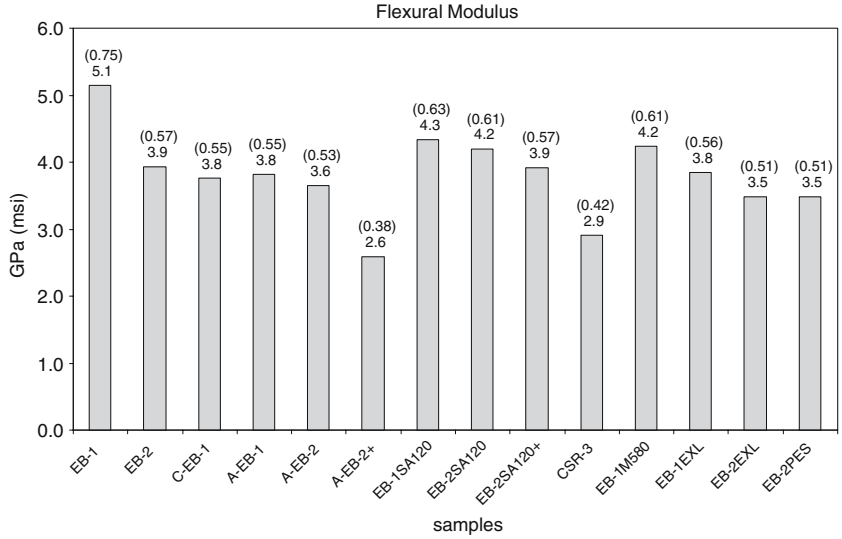

Fig. 18 Flexural moduli of all specimens in GPa; values in parentheses in msi

following samples may be considered statistically valid since they derive from at least five specimens: EB-1, A-EB-1, and A-EB-2. Other values than those originated mostly from at least three specimens. Details are covered later in this chapter with the explanation of the G_{Ic} values.

The EB-1 averaged around $0.7 \pm 0.09\,\mathrm{MPa}\sqrt{\mathrm{m}}$ and the EB-2 achieved a toughness of $0.9 \pm 0.17\,\mathrm{MPa}\sqrt{\mathrm{m}}$. The addition of 10% ATBN rubber improved the toughness in all systems; the A-EB-1 achieved $0.9 \pm 0.20\,\mathrm{MPa}\sqrt{\mathrm{m}}$ and the A-EB-2 1.2 ± 0.13 $\mathrm{MPa}\sqrt{\mathrm{m}}$. The A-EB-2+ contained 20% of the toughener and reached the second highest fracture toughness value with $1.3 \pm 0.17\,\mathrm{MPa}\sqrt{\mathrm{m}}$. The CTBN rubber in the C-EB-1 matched the fracture toughness of the ATBN-toughened sample with $0.9\pm\ 0.0\,\mathrm{MPa}\sqrt{\mathrm{m}}$. However, only 2 out of 10 different C-EB-1 specimens were tested since the brittleness did not allow the successful initiation of starter cracks in any of the other prepared specimens. Although the mean numerical value showed toughness comparable to the A-EB-1, the result could not be repeated. It was undoubtedly a far more brittle system than the one toughened with ATBN. The increased toughness was expected but it took place at a smaller scale than when applied to epoxy resins [11].

In the group of thermoplastics, the PPO® SA120 was studied in all systems at a 10% ratio. The EB-1SA120 achieved $0.6 \pm 0.37\,\mathrm{MPa}\sqrt{\mathrm{m}}$ and the EB-2SA120 $1.0 \pm 0.12\,\mathrm{MPa}\sqrt{\mathrm{m}}$. The slight improvement in toughness encouraged the investigation of 20% in the EB-2 resin where the value $0.6 \pm 0.07\,\mathrm{MPa}\sqrt{\mathrm{m}}$ dropped below that of the neat EB-2 resin. The PES was only studied in the EB-2 resin and did not change the fracture toughness. The numeral value was identical to

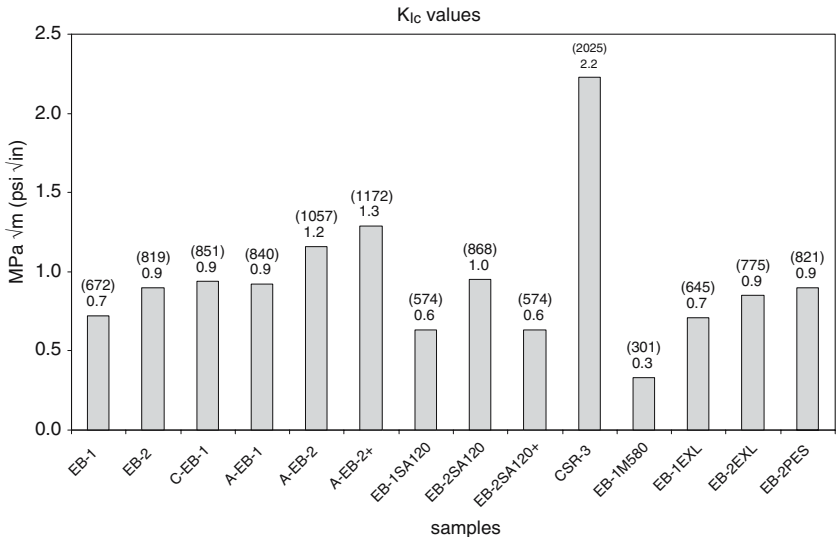

Fig. 19 Plain strain fracture toughness of all specimens in $\mathrm{MPa}\sqrt{\mathrm{m}}$; values in parentheses in $\mathrm{psi}\sqrt{\mathrm{in}}$

the neat resin with $0.9 \pm 0.30\,\mathrm{MPa}\sqrt{\mathrm{m}}$, which most likely was caused by the complete separation of the toughener from the matrix prior to cure at bulk level. The PES formed a circle inside the benzoxazine resin which surrounded the thermoplastic. Thus it was no surprise that the samples did not show any increase in toughness. The performance of the thermoplastic tougheners did not meet our expectations since we were aware of some toughness improvement with epoxy resins [2].

The core–shell polymers achieved the following K_{Ic} values: the CSR-3 had by far the highest value with $2.2 \pm 0.0\,\mathrm{MPa}\sqrt{\mathrm{m}}$ but it must be kept in mind that the starter crack here was sawed in with a razor blade since the authors experienced major difficulties with the tapping method which could not be overcome. Moreover, the almost thermoplastic behavior was probably the result of the 26.5% core–shell rubber compared to the other samples that contained only 10% toughener. The EB-1M580 showed a drop in fracture toughness to $0.3 \pm 0.12\,\mathrm{MPa}\sqrt{\mathrm{m}}$, the EB-1EXL resulted in a value of , and the EB-2EXL achieved . Due to the major difficulties in the experimental part with these formulations, a comparison to other worker's results would not be of great use. We know that Sue found better results with epoxies [8].

Frequently, researchers as well as industry workers refer to the strain energy release rate. The ASTM standard offers a conversion to the strain energy release rate. The results of the G_{Ic} values are presented in Fig. 20.

In Fig. 20 a numeric average of all received mode I toughness data is presented. The deviation of each value will be given although it has to be kept in mind that by the conversion with Eq. 3, unknown errors are inherent due to the above mentioned assumptions for Poisson ratio and the usage of a flexural instead of a tensile modulus. The baseline was set by the EB-1 system that was used as a control during every sample run. The mean value for the strain energy release rate of the EB-1 system was determined to be 88 ± 8 J/m^2. Note that the various systems did not deliver statistically valid numbers due to their brittleness that resulted in unsuitably initiated crack lengths. Following Srawley [18], although these values are invalid for the purposes of the ASTM D 5045-96 test method for monotonic loading, those wider ranges of a/W ratios can be used for fatigue crack propagation. Srawley [18] presented a polynomial equation in which the deviations in the dimensionless factors occur in the first digit behind the decimal point. The authors therefore concluded that, as a first indication of the toughener's performance, using the received values was adequate.

The C-EB-1 resin was prepared twice and each time only a single specimen could be prepared with a/W-ratios of 0.70 and 0.40 for the initiated cracks. The values received averaged to 173 ± 6 J/m^2.

The EB-1M580 core–shell toughened resin performed poorly with an average value of 25 ± 22 J/m^2. The used a/W ratios within the three specimens were between 0.55 and 0.78.

Both the EB-1SA120 and the EB-1EXL system achieved a G_{Ic} value of 123 J/m^2, the former with a scatter of 84 J/m^2 and the latter with one of 67 J/m^2. The PPO® toughened specimens were tested with a/W ratios varying from 0.39 to 0.76 while the best value for energy release rate, 230 J/m^2, was achieved with an a/W ratio of 0.47, which is exactly in the proposed range of the ASTM D 5045-96 of $0.45 < a/W < 0.55$. The

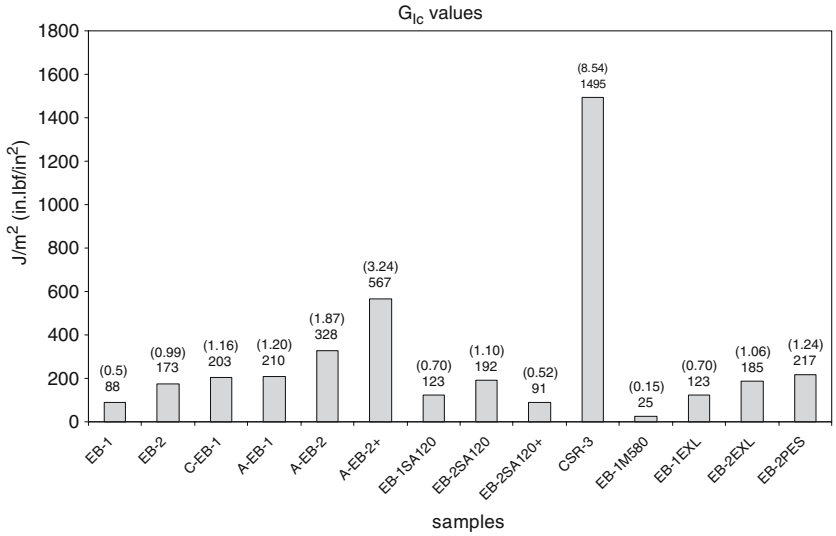

Fig. 20 Strain energy release rates of all specimens in J/m^2; values in parentheses in lbf in./in.^{2}

system with the Paraloid^{TM} EXL 2330 had cracks initiated at a rate of 0.54–0.72.

A significant increase in fracture toughness was achieved by adding ATBN 1300x16 to the EB-1. First results encouraged the accomplishment of a valid statistic, where a strain energy release rate of 210 ± 81 J/m^2 was determined.

The CSR-3 sample achieved by far the highest value within all tested samples. Yet as already mentioned, it was not possible to initiate a starter crack by tapping with a razor blade and the crack was made by sawing with the blade instead. Still it remained so difficult to derogate the material that the resulting crack lengths had an a/W ratio of 0.37 and 0.38 which is of course below the postulated 0.45. However the authors were of the opinion that the CSR-3 possessed a greatly increased fracture toughness at least at the given ratio of 26.5% toughener. The numerical G_{Ic} value of 1,495 ± 22 J/m^2 was an average of two specimens and could therefore only be taken as a rough qualitative indication. Further investigations remain subject to nondisclosure.

The EB-2 endued a strain energy release rate of 173 ± 63 J/m^2 which was already almost double that of the EB-1. Starting from a higher base, it was not surprising that the effect of ATBN rubber resulted in a greater value of 328 ± 72 J/m^2 with 10% toughener and of 567 ± 140 J/m^2 with 20% toughener. A valid statistic was prepared with the A-EB-2 sample, i.e. 10% toughener, where the above mentioned value was received with a/W ratios between 0.47 and 0.85. The three specimens with 20% ATBN modifier had an a/W ratio of 0.48–0.67.

The EB-2SA120 sample did not significantly change the fracture toughness; indeed the crack initiation was found to be difficult due to the free length of path the tapped crack took once started. Yet the strain energy release rate was 193 ± 41 J/m^2. Moreover it was interesting that the cured sample remained translucent and therefore encouraged the study of EB-2SA120+ with 20% PPO® which resulted in a profound loss in fracture toughness. The average of 91 ± 31 J/m^2 was comparable to the level of the neat F-a type benzoxazine. Still the sample remained translucent. Due to the brittleness of the sample, only two specimens could be successfully prepared and tested at a/W ratios of 0.56 and 0.71. Other workers experienced an increase in toughness value when PPO was added as a toughener in epoxy resins [19].

The sample with PES as a thermoplastic toughener achieved an average G_{Ic} value of 217 ± 122 J/m^2. However the results were measured with a/W ratios of 0.64, 0.75, and 0.82 and the second specimen achieved an energy release rate of 345 J/m^2. It was observed that in this case, the crack ran straight through an area containing predominantly a macroscopic phase of PES, while the cracks in the other two samples propagated through a two-phase area.

The core–shell polymer Paraloid^{TM} EXL 2330 was tested in both benzoxazine resins, F-a type and B-m type. The strain energy release rate found in the EB-2 system varied between 173 ± 63 and 186 ± 50 J/m^2. This time the inserted failures ended with a/W ratios between 0.54 and 0.63, which was close to the postulated range.

Structure–property relationships/microscopic studies

This section shows SEM images of fractured surfaces that were tested in a three-point bending mode to determine the K_{Ic} and G_{Ic} values. All images were taken at an electron acceleration of 20 kV and the cracks propagated from right to left.

In all benzoxazine resins toughened with ATBN a second phase could be observed. In A-EB-1 (Fig. 21), the reactive liquid rubber showed an average particle size distribution around 1–1.5 μm and appeared homogeneously dispersed in the thermosetting resin forming circular inclusions. The fractured surfaces showed stress-whitening and cavitation. The A-EB-2 (Fig. 22) system achieved a higher K_{Ic} value than the A-EB-1. The particle size of the second phase was around 1 μm and the shape appeared not quite circular but rather stretched. The number of crack layers was similar to the A-EB-1. At an amount of 20% ATBN in the B-m type benzoxazine (Fig. 23), the surface appeared as a mixture with no visible second phase. An

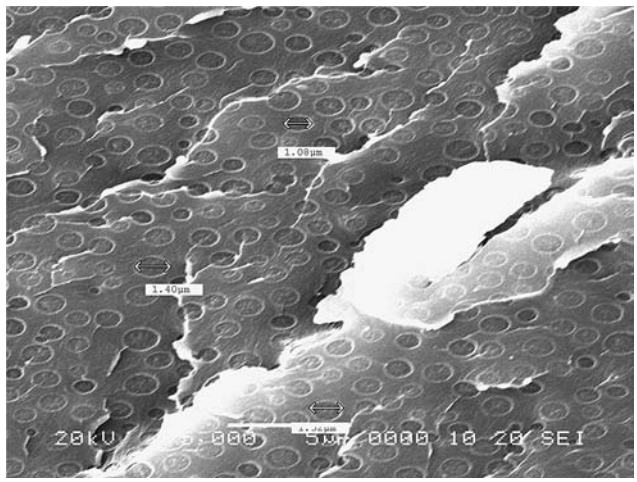

Fig. 21 SEM image of EB-1 resin toughened with 10% ATBN 1300x16 (magnification of 5,000×)

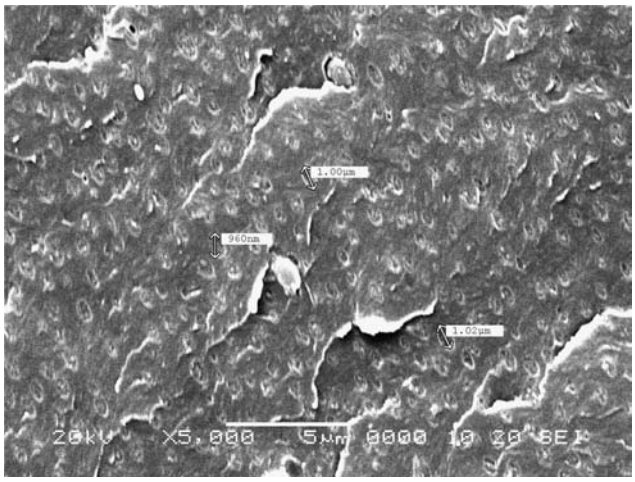

Fig. 22 SEM image of EB-2 system toughened with 10% ATBN 1300x16 (magnification of 5,000×)

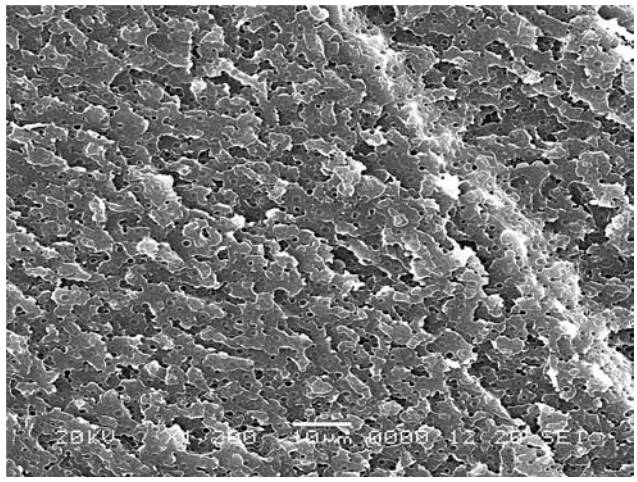

Fig. 24 SEM image of EB-1 system with 10% CTBN rubber (magnification of 1,200×)

increasing number of crack layers was found to be responsible for the higher fracture toughness.

In the CTBN toughened F-a type resin the particle size distribution was also found at an average of 1–1.5 μm. Although the rubber was well dispersed as a second phase and the flake-like surface in Fig. 24 gave evidence of the development of multiple planes for crack propagation the crack resistance was low as discussed in the previous chapter. At higher magnification (see Fig. 25), a glassy, solid surface was visible without any signs of toughening mechanisms like crazing or rubber bridging. Some particles show cavitation effects, but apparently the crack propagated along the matrix without any significant influence of the second phase regarding toughening mechanisms. Addressing the shape of the particles, similar results to those observed in epoxies by Kunz et al. [11] were found. They reported sharp interfaces in CTBN-toughened specimens versus a diffuse appearance of the irregularly shaped particles in the ATBN-modified matrix. In their case, no difference in toughness improvement was found between the two rubbers. This was certainly not true in the present project where the fracture toughness increased in all systems with the addition of ATBN rubber.

The EB-1SA120 (Fig. 26) showed homogeneously dispersed particles of an average particle size around 1 μm in diameter with a very narrow distribution. The fractured surface showed particles that were either cut through, debonded, or torn out, leaving voids behind. The crack propagation took place in various layers

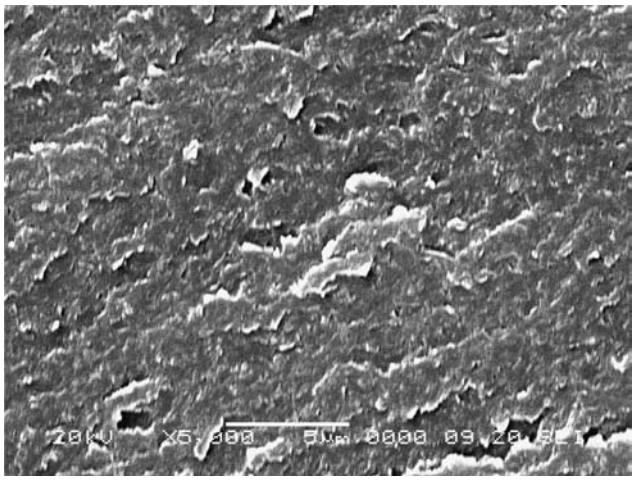

Fig. 23 SEM image of EB-2 resin toughened with 20% ATBN 1300x16 (magnification of 5,000×)

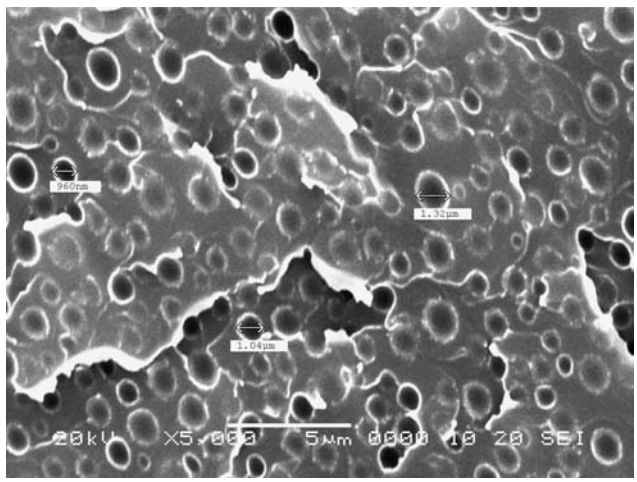

Fig. 25 SEM image of EB-1 system with 10% CTBN rubber (magnification of 5,000×)

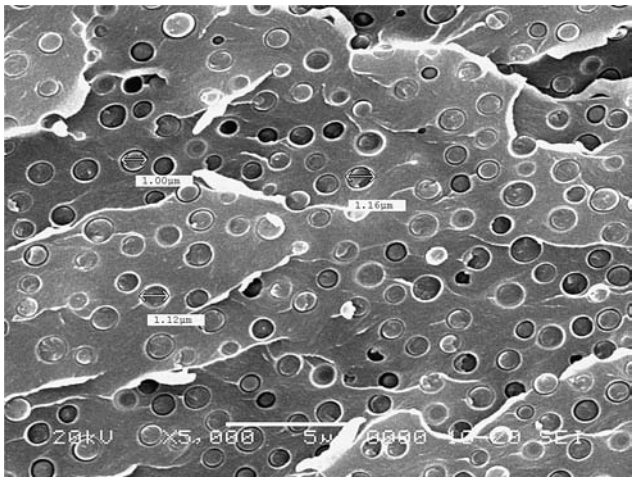

Fig. 26 SEM image of EB-1 system with 10% PPO® SA120 (magnification of 5,000×)

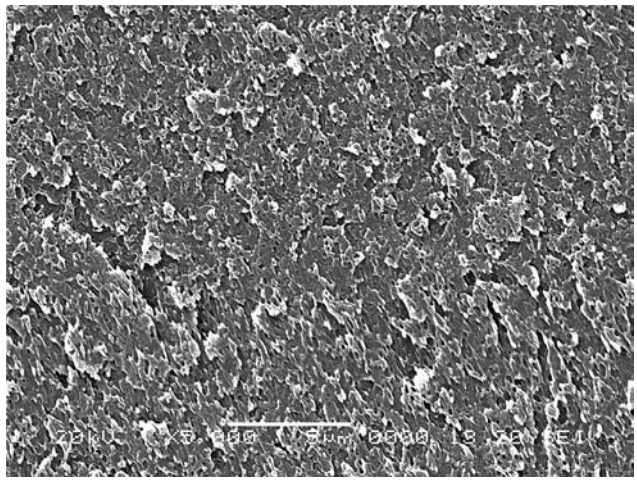

Fig. 28 SEM image of EB-2 system with 20% PPO® SA120 (magnification of 5,000×)

initiated by the added particles. The K_{Ic} value of $0.6\,MPa\sqrt{m}$ was lower than the neat resin fracture toughness whereas the calculated G_{Ic} was higher with 123 J/m^2.

The EB-2SA120 (Fig. 27) showed a completely different surface: Here the particles were by an order of magnitude smaller and the image shows mainly voids and several planes along which the crack path was visible. These observations were found to be responsible for a slightly increased failure resistance. Apparently the PPO® SA120 was soluble in the B-m type benzoxazine and the authors assume that it reacted with the backbone of the matrix. This was also consolidated by the fact that the cured specimens remained translucent. The authors regret that there is no evidence for the suggested phenomena.

The EB-2SA120+ with 20% toughener (Fig. 28) showed a significant loss in fracture toughness. The micrograph showed less voids and the particles were again smaller than those observed in the EB-2SA120 (Fig. 27). Again numerous layers left behind by the propagating crack were observed. Although no flaws could be identified with the used method, it may be assumed that very small particles interfering with the crack were responsible for the build-up of the different planes.

The fractography of the core–shell toughened samples showed fairly different images. The Paraloid™ EXL 2330 with the F-a type benzoxazine (Fig. 29) appeared homogeneously dispersed at an average particle size around 1 µm with a small distribution. Many particles acted as flaws as previously observed in

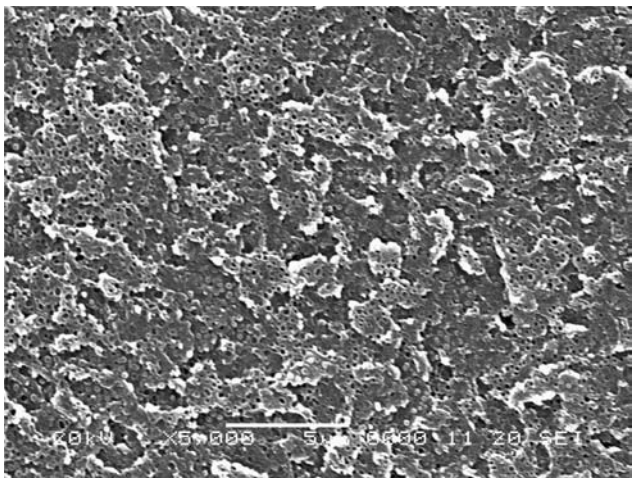

Fig. 27 SEM image of EB-2 system with 10% PPO® SA120 (magnification of 5,000×)

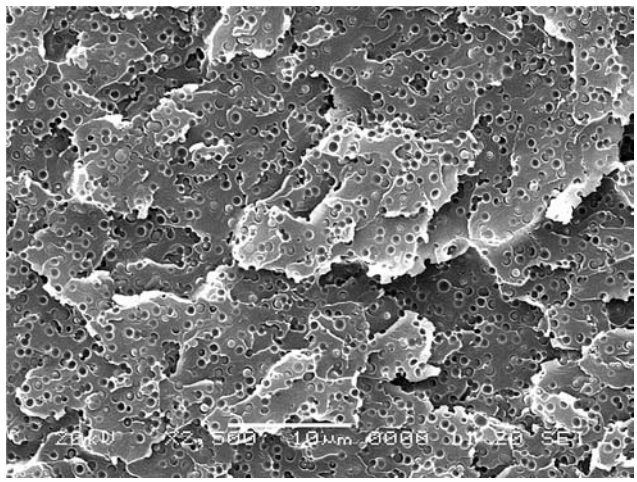

Fig. 29 SEM image of EB-1 resin with 10% Paraloid™ EXL 2330 core–shell modifier (magnification of 2,500×)

samples with rubber modifier. The crack propagation therefore took place on multiple planes. A mixture of cavitation and particle cutting was observed as failure cause.

In the EB-1M580 (Fig. 30) the particle size was found to be smaller, around 0.5 μm, with an increased distribution. A decrease in K_{Ic} value as well as in G_{Ic} value was found. Although some cavitation was visible, the majority of the particles were cut through and remained debonded from the matrix as rigid, white-colored flaws for crack plane initiation.

In the CSR-3 (Fig. 31) no particles were observed with the SEM. Yet multiple crack layers clearly indicated the existence of many particles acting as flaws. It was assumed that the excellent toughness of this material was caused by a synergism of crack deflection and shear yielding mechanisms as well as particle cavitation. To propagate, the crack had to overcome numerous different layers initiated by small particles of approximately 100 nm diameter. Their small distribution as well as their constant interparticle distance could combine the latter effect with Lange's line tension mechanism that forces cracks to bow [20]. Due to the rubbery core, the occurrence of crazing should not be excluded, although in this project no evidence could be given with the applied investigation methods.

The EB-2EXL system (Fig. 32) showed an inhomogeneously dispersed second phase in the matrix. The core–shell modifier particles were obviously removed during the fracture event, leaving empty cavities behind on the surface with an average size of below 1 μm. The fracture toughness was similar to that of the neat resin.

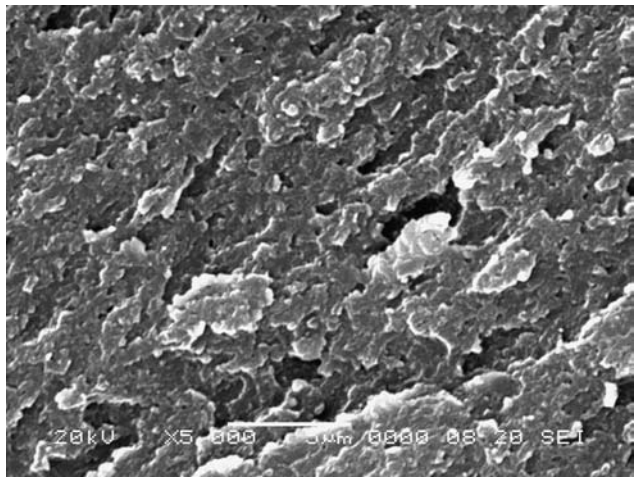

Fig. 31 SEM image of EB-1 resin with 26.5% of the CSR-3 modifier (magnification of 5,000×)

Summary and conclusion

To summarize the previous chapter it can be stated that the B-m type benzoxazine resin performed best in light of the goals postulated initially. The higher glass transition temperature of the neat resin as well as the higher flexural strength and fracture toughness were advantageous while the problems occurring from the higher viscosity and the lower flexural modulus were considered disadvantageous. Another advantage was that for complete curing of the EB-2 resin no catalyst was necessary as proved by DSC analysis. The catalyst increased the moisture absorption of the samples and furthermore, due to the catalyst having to be completely dissolved in the F-a type benzoxazine, an extended heat exposure had to be undertaken during resin processing.

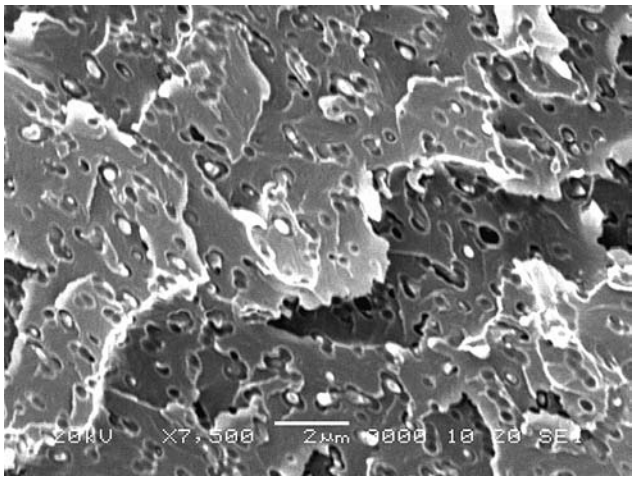

Fig. 30 SEM image of EB-1 resin with 10% Kane Ace M580 (magnification of 7,500×)

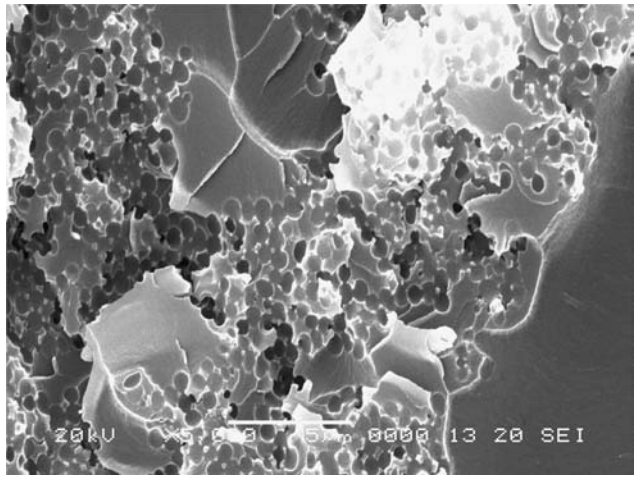

Fig. 32 SEM image of EB-2 resin with 10% Paraloid™ EXL 2330 (magnification of 5,000×)

Although the main focus was put on the value gained in strain energy release rate, i.e., G_{Ic}, the other properties should maintain their value while simultaneously improving the crack resistance.

The thermoplastic toughness modifier PES was incorporated through a solvent route. While the removal of the DMF worked well with the EB-1 system which was proved by FTIR, DSC, and TGA, this was not true in the EB-2 system. An undetermined amount remained, probably around 5%, that possibly dissipated during the curing process but still would not be acceptable for aerospace applications. After cure only a minor amount of PES was dispersed in the resin while approximately 90% of the thermoplastic remained as separate phase. Therefore specimens tested had different ratios of toughener and resin and hence the results varied significantly. Only vague estimates were found: an improvement of G_{Ic} value, a decline of flexural properties, and higher moisture absorption.

A solventless incorporation was realized with PPO® as a toughener. An increase in G_{Ic} value was achieved with both resin types when PPO® SA120 was added at 10% by weight. An increased content of 20% lowered the value in the EB-2 system. Further in the EB-2 resin, the moisture absorption decreased when the ratio was moved to higher thermoplastic content. Remarkable was the fact that in the EB-1 system the thermoplastic agent turned the resin opaque whereas in the EB-2 system the resin remained translucent. Yet both systems showed a second phase morphology consisting of particles with an average size of 1–2 μm. The modifier caused a noticeable decrease of flexural properties, especially in the EB-2 system at 20% ratio.

As mentioned previously, the CTBN rubber did not succeed as a toughener in the benzoxazine resins. Instead, the ATBN rubber performed excellently with EB-1 and EB-2 although the responsible mechanism remained unclear. The combination of mechanisms like cavitation and shear yielding was doubtful since the micrograph of the A-EB-1 system showed no cavities.

The reason for the formation of different particle geometries when ATBN or CTBN modifiers are used, is not understood, but the authors assumed that the different chemical reactivity of the rubbers may have been responsible. Furthermore, the observation of an increasing T_g at an increasing rubber content led to thoughts of chemical reactions during cure in addition to physical interactions by the dispersion of a second phase in a matrix. Finally, the excellent hot/wet performance of the EB-2 system with 20% ATBN suggested the occurrence of chemical reactions that reduced the water absorption of the toughened resin.

Inside their own group the core–shell polymers acted differently. While the Kane Ace M580 did not increase the toughness, the Paraloid™ EXL 2330 showed some improvement in the EB-1 system. Much had to be attributed to the processing of these samples. Particle agglomeration occurred in the EB-2-EXL as shown in Fig. 32, and the heat history of the resins due to the applied shear rate was difficult to determine. Moreover, the consistencies of the two commercial products were not known in detail. Especially the Kane Ace M580 was probably designed with respect to the group of all-acrylic impact modifiers and hence possessed major impact on weatherability rather than toughness improvement. The CSR-3 polymer was incorporated via an improved processing route without affecting the resin's neat properties by overheating. The small particle size distribution and the even interparticle distance were assumed to be responsible for the superior properties of the sample. However, the toughener was added at a significantly higher percentage than all other modifiers and hence direct comparison is not appropriate.

The properties observed gave hopes for the usage of the benzoxazine resins in structural adhesives or liquid molding applications. Unpublished results by Henkel Loctite Aerospace Company underline the use in composite laminates by a satisfying compatibility of the benzoxazine resins with carbon fibers. It can be stated that the benzoxazine chemistry has many advantageous properties compared to phenolic or epoxy resins, especially multifunctional epoxy resins. The benzoxazine resins had to be processed at elevated temperatures but this is also true with epoxies where temperatures may be even higher. Benzoxazines also do not require any hardeners or accelerators. Although the flexural strength and the T_g, dry are lower than those of multifunctional epoxies, the benzoxazines possess higher initial toughness and higher flexural as well as tensile moduli. The water absorption is significantly lower (1% vs. 4%) and hence the performance of the hot/wet conditioned specimens did not vary as much compared to that of the dry specimens as with epoxies. Other benefits are the lack of exothermal potential and the near-zero shrinkage during cure [12].

With respect to primary structural aircraft components, benzoxazine resins offer service temperatures above 120 °C where especially diglycidyl ether of bisphenol-A (DGEBA) resins are not satisfactory [21].

Although it was difficult to toughen the resins effectively, especially since some of the well-known modifiers in epoxy resins acted differently in the experiments with the benzoxazines, the received values can compete with those of highly cross-linked epoxies. One reason for the variation may be hidden in a different solubility parameter.

Beyond the focus of this study were advanced formulations that prevent the swelling behavior of the benzoxazines above 220 °C. With respect to commercial products this problem will have to be solved by appropriate chemistry. Initial screening work with polyetheretherketone (PEEK^{TM}) fibers points to possible applications in pastes or adhesives. Ishida [22] studied the impact of poly(ε-caprolactone) with promising results. Since success in blending benzoxazine and epoxy resins has been reported, the incorporation of an epoxy-terminated liquid rubber (ETBN) is self-displayed. Finally, combinations of toughening agents studied in the present project such as ATBN rubber and alumina powder may have a successful outcome. Further research will be necessary to determine the true mechanisms responsible for the structure–property relationships found within this work.

Acknowledgements The authors would like to thank Mr. Raymond S. Wong of Henkel Loctite Aerospace for providing laboratories in the R&D facilities as well as equipment and materials free of charge. Special thanks belong to Mr. Stanley L. Lehmann for sharing his invaluable experience and advice. The authors would like to thank numerous scientists at the Henkel Loctite Aerospace R&D center for technical assistance and illuminating discussions. The authors wish to thank Dipl.-Ing. (FH) Dietrich Sülthaus from the department of Polymer Engineering at Bayreuth University for his encouragement. Finally the authors wish to thank Miss Martha L. Gurtz for her assistance in reviewing the manuscript. This work was partially funded by the department of Polymer Engineering at Bayreuth University.

References

1. Agag T, Takeichi T (2002) High Perform Polym 14(2):115
2. Renner M, Altstädt V, Döring M, Merz T, Räckers B (2000) 32nd International SAMPE Technical Conference, vol 32, pp 619–632
3. Bucknall CB, Yoshii T (1978) Br Polym J 10(1):53
4. Yee AF, Pearson RA (1986) J Mater Sci 21:2462
5. Pearson RA, Yee AF (1986) J Mater Sci 21:2475
6. Pearson RA, Yee AF (1989) J Mater Sci 24:2571
7. Pearson RA, Yee AF (1991) J Mater Sci 26:3828
8. Sue HJ, Garcia-Meitin EI, Pickelmann DM, Yang PC (1993) In: Riew CK, Kinloch AJ (eds) Toughened plastics I. Science and engineering. Advances in Chemistry Series 233. ACS, Washington, DC, pp 259–291
9. New type of thermosetting resin: Benzoxazine, presentation of Shikoku Corporation, confidential
10. Noveon^{TM} (B.F. Goodrich Company) (1998) Hycar® reactive liquid polymers: ATBN 1300x16, and CTBN 1300x13, Product data sheets
11. Kunz SC, Sayre JA, Assink RA (1982) Polymer 23:1897
12. Ishida H, Allen DJ (1996) J Polym Sci: Part B: Polym Phys 34:1019
13. Standard test method for flexural properties of unreinforced and reinforced plastics and electrical insulating materials, ASTM D 790-97
14. Standard test method for plane-strain fracture toughness and strain energy release rate of plastic materials, ASTM D 5045-96
15. Bucknall CB (1977) Toughened plastics. Applied Science Publishers Ltd
16. Hodgkin JH, Simon GP, Varley RJ, (1998) Polym Adv Technol 9(1):3
17. Shaw SJ (1994) In: Collyer AA (ed) Rubber toughened engineering plastics. Chapman & Hall, pp 165–209
18. Srawley JE (1976) Int J Fract Mech 12:475
19. Wu SJ, Tung NP, Lin TK, Shyu SS (2000) Polym Int 49(11):1452
20. Lange FF (1970) Philos Mag 22:983
21. Altstädt V (1991) Makromol Chem Macromol Symp 50:137
22. Ishida H, Lee Y-H (2001) Polymer 42:6971